JOURNAL OF PROPULSION AND POWER
Vol. 22, No. 1, January–February 2006

Unsteady Quasi-One-Dimensional Nonlinear Dynamic Model of Supersonic Through-Flow Fan Surge

Jacques C. Richard*
Texas A&M University, College Station, Texas 77843-3141

This paper presents the results of a computational fluid dynamic model of a supersonic through-flow fan (STF) in supersonic surge. The phenomenon of surge is well known for subsonic turbomachinery. However, for supersonic turbomachinery like the STF, a special type of supersonic surge occurs in which a shock oscillates through the fan, alternating locations between upstream and downstream of the fan. It is also possible for a shock to remain in a fan stage. This analysis focuses on the development of supersonic surge resulting from overpressuring the fan. A model of the STF was constructed around its steady-state experimental performance map using an existing unsteady, quasi-one-dimensional, inviscid, compressible flow code. An exit boundary condition was specified for the overpressuring that forces the shock to move upstream and interfere with normal fan operation. The effects of that interference, including a shock oscillating across the fan, are discussed.

Nomenclature

A	=	cross-sectional area through which flow passes
c_p	=	specific heat at constant pressure
c_v	=	specific heat at constant volume
E	=	internal energy of working fluid
F	=	external force applied to working fluid
FAC	=	factors that appear in turbo machinery momentum source term
H	=	specific enthalpy (enthalpy per unit mass)
L	=	length
M	=	local Mach number
M_s	=	mass injected into or extracted from working fluid (mass equation source term)
MR	=	mass ratio term in turbomachinery momentum source term
p	=	local static pressure
p_t	=	local total pressure
Q	=	energy going into or out of the working fluid
R	=	gas constant
r	=	radius
T	=	local static temperature
T_t	=	local total temperature
t	=	time
u	=	axial velocity (only component for quasi-one-dimensional flow assumption)
x	=	local axial position
γ	=	ratio of specific heat at constant pressure to that at constant volume
ρ	=	local working fluid density

Subscripts

cowl	=	relating to the cowl as in r_{cowl} for cowl radius
exit	=	fan exit (at stator trailing edge)
i	=	index in discretized form of differential equations
inlet	=	fan inlet (at fan face or rotor leading edge)
max	=	largest value of a quantity as in $r_{\text{cowl,max}}$ for maximum cowl radius (24 in. or 60.96 cm)
O	=	property upstream of inlet used for nondimensionalizing main variables
plenum	=	pertaining to the plenum
ref	=	reference variable used for nondimensionalizing variables
s	=	source term
stage	=	belonging or referring to a variable that relates to the fan stage

Received 1 November 2004; revision received 9 June 2005; accepted for publication 22 June 2005.

*Research Associate Professor, Aerospace Engineering, Mail Stop 3141; richard@aero.tamu.edu. Senior Member AIAA.

I. Introduction

In pursuing the goal of faster and longer-range aircraft to prepare for the rapid growth in air traffic across the Pacific and Atlantic, economically viable supersonic passenger transports are needed to avoid the costliness that led to the retiring of the Concorde. Indeed, supersonic transports are of more than passing interest. NASA and business-jet manufacturers have feasibility studies of some type of supersonic aircraft, for example, the Quiet Supersonic Business Jet[1–5] and DARPA studies hypersonic cruise vehicles. Supersonic air vehicles would be well served by an all-supersonic engine using a supersonic inlet and supersonic through-flow fan (STF and sometimes referred as STFF) that is receiving renewed interests.[6,7] In an STF, there is no deceleration of the flow to subsonic needed thereby reducing associated strong shock losses. This fan would be more efficient with higher pressure ratios, reduced shock losses (as smaller and weaker oblique shock waves are obtained instead of stronger normal shocks[8–12]), and a shorter inlet allowing for a lighter vehicle. Franciscus[8] summarized the development of STF-based propulsion systems and compared them to conventional engines (Fig. 1). The STF is usable with either a subsonic or supersonic gas generator core. Schmidt et al.[9] pointed out the possibility of obtaining higher pressure ratios with an STF and presented the design criteria for the proof-of-concept fan that had a total pressure ratio of 2.45 at the design Mach number of 2.0 at the fan face. The important design criteria include 1) maintaining constant tip and hub radii throughout the fan stage to limit three-dimensional effects (only two-dimensional tools were available at the time of the designs in Franciscus[8] and Schmidt et al.[9]); 2) ensuring supersonic through-flow throughout the compression system with weak shock waves and ensuring the capture of the shock structure within the bladed passages; and 3) adjusting pressure gradients in key flow regions for minimizing shock strengths in internal compression and expansion systems. The STF's steady-state aerodynamic performance is documented.[8–12]

Although the performance of the STF is encouraging, are they also susceptible to instabilities that can affect subsonic vehicles?[13–16] For subsonic and transonic turbomachinery, the phenomena of surge and stall are well understood.[9] In supersonic surge, a shock system can exist in which a shock oscillates through the fan, alternating

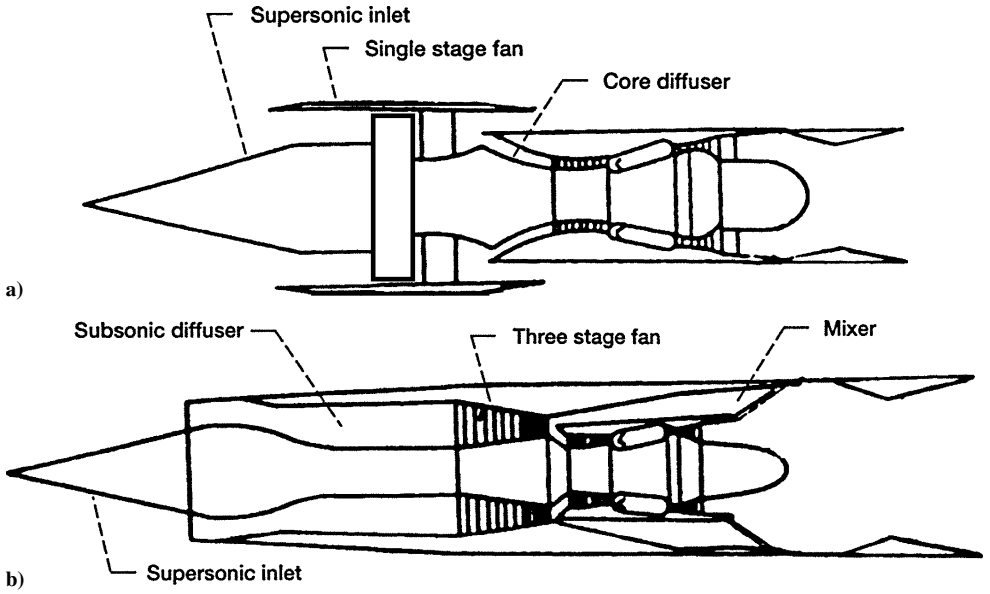

Fig. 1 Supersonic engine design options: a) STF engine configuration[3] vs b) conventional engine.

Table 1 Supersonic through-flow fan design parameters

Parameter	Value
Total pressure ratio	2.45
Weight flow rate, lb/s	31.5
Inlet axial Mach number	2.0
Rotor tip speed, ft/s	1500
Rotative speed, rpm	17,180
Tip diameter, in.	20
Hub-to-tip ratio	0.7

locations between upstream and downstream of the fan. It is even possible for a shock to remain in the fan.

To identify and characterize the supersonic surge characteristics of an STF stage, an analysis model[17–19] was constructed as part of the NASA STF dynamics and controls research program.[18–20] The model required a steady-state fan performance map that can be obtained from experimental data or from computational-fluid-dynamic turbomachinery design codes. Perturbations are imposed that might be upstream or downstream in the Mach number, pressure, flow rate, or nozzle-diffuser geometry or a combination thereof. In an engine, these perturbations can arise from combustion instabilities or inlet variations. Furthermore, altitude and freestream changes can also lead to perturbations depending on the engine-inlet configuration. To encourage the occurrence of supersonic surge, the exit Mach-number boundary condition in the analytical model was reduced, as a throttling mechanism with increasing backpressure, which then forced a shock to move upstream toward the fan and interfere with its normal operations.

II. Configuration of STF Stage in Test Cell Analyzed

The design of the STF is documented in detail,[9–12] and only a brief description of the relevant design parameters is presented here for completeness. The overall design parameters are listed in Table 1. The STF stage was designed to operate with supersonic axial velocities from its inlet to its exit. An experimental layout or test package is shown with the flow-path geometry as modeled presented in Fig. 2 with key regions highlighted (to be specified later), as the centerbody moves, according to where notable results will be discussed. The horizontal axis represents the centerline of this axisymmetric test section. For subsonic flow, the downstream diffuser was opened to the maximum position, and the inlet Mach number (and also flow rate) was controlled by the upstream nozzle. The overall performance of this baseline test stage is shown in Fig. 3.

Two cases of predicted performance of the fan startup to operating condition at a fan face Mach number of 2.0 and 1.5 are examined. Case 1 simulates the fan being operated to design RPM before it is unstarted. Case 2 examines the fan when unstarted at design rpm with a fan face Mach number of 1.5. The ramifications on control of STF-based engines are discussed.

III. Analytical Model

The flow through the STF in the test cell is primarily axial and quasi one dimensional (spatially and temporally varying cross-sectional flow areas). The flow is also compressible and assumed inviscid (viscous effects are in the nonsimulated boundary layer assumed negligible compared to the full flowfield dimension for this analysis). The governing equations are

$$\frac{\partial}{\partial t}(\rho A) + \frac{\partial}{\partial x}(\rho A u) = M_s \tag{1}$$

$$\frac{\partial}{\partial t}(\rho A u) + \frac{\partial}{\partial x}[(p + \rho u^2)A] = p\frac{\partial A}{\partial x} + F_s \tag{2}$$

$$\frac{\partial}{\partial t}(EA) + \frac{\partial}{\partial x}[(p + E)Au] = -p\frac{\partial A}{\partial t} + Q_s \tag{3}$$

where $E = \rho(c_v T + u^2/2)$. The analysis assumes the flow is thermally and calorically perfect such that the perfect-gas equation of state can be used as $p = \rho RT = (\gamma - 1)(E - \rho u^2/2)$. These equations are said to be in weak conservative form because the area change terms and possible sources (or sinks) of mass, momentum, and energy are on the right-hand side. These equations are solved numerically using a split-characteristics finite difference algorithm[17] with user-specified spatial grid size and time-step size in the Large Perturbation Inlet (LAPIN) code.

Key elements of the LAPIN code were modified to model supersonic inlet flowfields with external transfers of mass, momentum, and energy to the flowfield as source terms in the governing equations. The code includes the following: bleed and bypass capabilities; translating and collapsing centerbody and other geometric variables of duct segments; start, unstart, and restart transient capability; and the ability to approximate axisymmetric or two-dimensional flow fields external to the inlet. The code incorporates mixed supersonic and subsonic flow regimes with one or more normal shocks as is typical of supersonic vehicle inlets. These features were incorporated via the source terms. The code has been verified against experimental data.[17] The code was modified to allow the effects of turbomachinery on the fluid mass, momentum, and energy to appear via the source terms with turbomachinery component properties linearly distributed over the grid points spanned by that component.

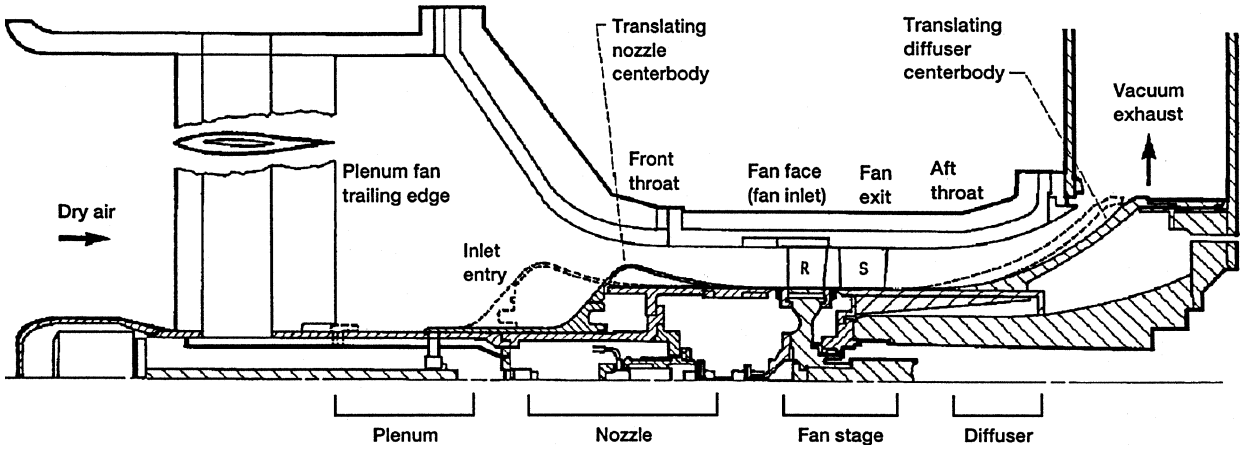

a) Cutaway side view of NASA test cell with STF fan stage

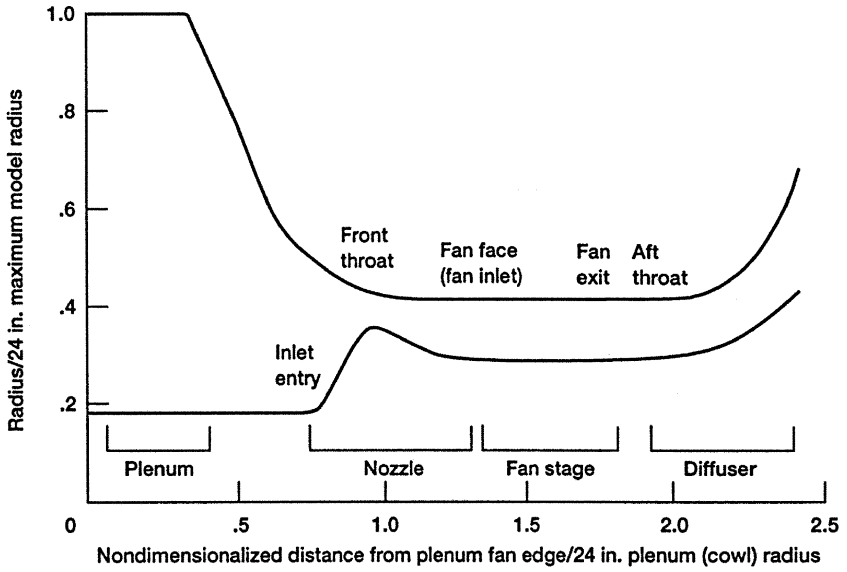

b) Computational domain of test cell and fan stage in model

Fig. 2 Computational model of STF in NASA Glenn Research Center test cell.[3,4] Note the flow path and geometry where key regions are noted for important output data.

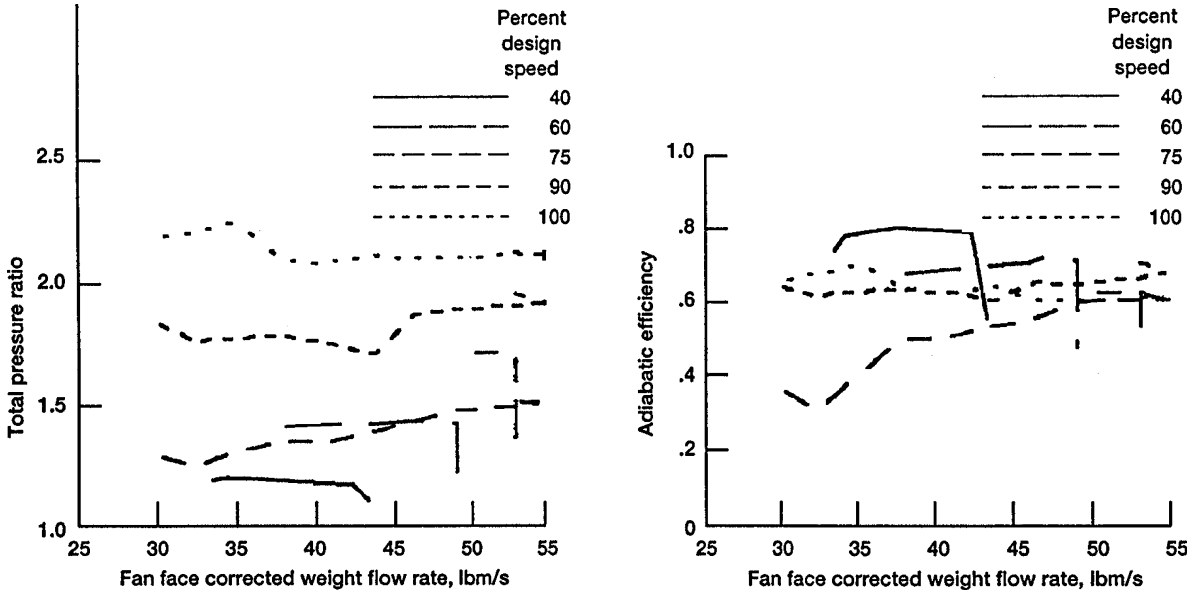

a) Total pressure ratio performance map

b) Efficiency performance map

Fig. 3 STF baseline test stage performance map used in model (with abscissa converted to corrected weight flow rate in lb/s or lbm/s).

The turbomachinery contributions to the source terms are added to the momentum and energy equations via F_s and Q_s. The flow takes the momentum imparted by the turbomachinery segment and the work that this segment does on the fluid. The total work per unit mass done by the fan stage is equal to the change in enthalpy across the stage[18]:

$$\Delta h = c_p(T_{t,\text{exit}} - T_{t,\text{inlet}}) \tag{4}$$

The primitive state variables are nondimensionalized as

$$\bar{\rho} = \frac{\rho A}{(\rho A)_{\text{ref}}}, \quad \bar{u} = \frac{u}{u_{\text{ref}}}, \quad \text{and} \quad \bar{p} = \frac{pA}{(\rho A u^2)_{\text{ref}}} \tag{5}$$

along with a reference length $L_{\text{ref}} = r_{\text{cowl,max}} = r_{\text{plenum}} = 24$ in., which is the largest outside radius of the modeled system in $A_{\text{ref}} = \pi(r_{\text{cowl,max}})^2$. The source terms are normalized using the freestream sonic velocity for the reference u_{ref}. The reference density is also evaluated at sonic conditions. Cole and Richard,[18] assuming adiabatic and thermally perfect conditions, use the relation between the freestream and freestream sonic velocity to obtain

$$\bar{Q}_{\text{stage}} = \frac{1}{2}\bar{\rho}_{\text{inlet}}\bar{u}_{\text{inlet}}\frac{\gamma+1}{\gamma-1}\frac{T_{t,\text{exit}} - T_{t,\text{inlet}}}{T_{t,O}}\frac{L_{\text{ref}}}{L_{\text{stage}}} \tag{6}$$

Equation (6) is the total energy source term that is linearly distributed over the fan stage grid points and the fan stage's length L_{stage}. The net change in fluid momentum imparted by the fan stage segment within a grid cell to the fluid within that cell (between stations i and $i+1$, the start and endpoints of the cell) is expressed as the normalized force per unit length as follows:

$$\bar{F}_{\text{stage}} = \left[\frac{(\bar{\rho}_i\bar{u}_i)^2}{\bar{\rho}_i}FAC_1 + \frac{(A_{i+1}+A_i)^2}{2A_i}\bar{\rho}_i FAC_2\right]\frac{L_{\text{stage}}}{x_{i+1}-x_i} \tag{7}$$

where

$$FAC_1 = (M_{i+1}/M_i)\sqrt{MR}\sqrt{T_{t,i+1}/T_{t,i}} - 1 \tag{8}$$

and

$$FAC_2 = (MR)^{\gamma/(\gamma-1)}(p_{t,i+1}/p_{t,i}) - 1 \tag{9}$$

in which

$$MR = \left\{1 + [(\gamma-1)/2]M_i^2\right\}\Big/\left\{1 + [(\gamma-1)/2]M_{i+1}^2\right\} \tag{10}$$

Previously developed turbomachinery performance map data evaluation and extrapolation routines[21] (see also Bruton, William M., "Data Alignment Program for AD100 Users," NASA internal unpublished report, NASA Glenn Research Center, 1989) were used to get values from the STF experimental performance map (Fig. 3). These routines linearly interpolate the turbomachinery total pressure ratio and efficiency from the STF performance map to compute the source terms. Linear extrapolation is used when the weight flow or corrected fan speed is out of the range of the current steady-state experimental map. In surge, the pressure ratio would fall to a low value[12] for the current model that is estimated[18,19] at the low end of the Mach number (or corrected weight flow rate) in the map of Fig. 3. In this figure, pressure ratio and efficiency approach 1.35 and 50%, respectively, as the Mach number is reduced (i.e., as the system is throttled back) while at high fan speed. These estimates assume the worst for the supersonic Mach number and fan speed ranges reported here. The estimates also alleviate any minor discrepancies that would result from extrapolating off the given map.

At this point, it should be noted that the normal steady-state STF operation could be in one or two modes, subsonic and supersonic. The map is different for each mode. The passage of a shock through the fan means moving between the two modes and, consequently, a change from one part of the map to the other. This could mean having to deal with a discontinuous source term. The Mach number is checked (i.e., greater or less than 1) at the fan face, and the appropriate part of the map is selected. Making this selection presents a difficulty if there is a shock between the fan face and fan exit. A dynamic map that accounts for a shock between the fan face and fan exit at any given time would serve best in later work.

More detailed modeling of the STF geometry should be done to see which flow patterns exist that could affect the fan map (e.g., blade-specific shock behavior). Other quasi-one-dimensional models of the stream-tube area specific to the volumes of fluid moving and turning about the STF blades might also do this, but the flow between the blades will always be multidimensional. Multidimensional models could show similar and other effects in greater detail (e.g., detailed shock structure, curvature, obliqueness and blade-specific shock locations) and even rotating stall or tip-clearance effects, but these would require more complex models.[22–25]

The equation for the work added to the flow [Eq. (3)] depends on enthalpy changes that are not affected by steady shocks. The shocks affect the equation for the momentum added [Eq. (2)] because this equation is more dependent on total pressure ratio, which changes across a shock. The grid-cell-distributed total pressure ratio [$p_{t,i+1}/p_{t,i}$ in Eq. (9)] is one that does not depend on the presence of a shock because the ratios are of terms on the same side of the shock.

IV. Rendering Model Compatible with STF Test Package

A large subsonic region [axial extent from 0 to –10 (unitless, code axial variable normalized using a 24-in. plenum maximum cowl radius)] is specified in front of the baseline fan and inlet system in the model test package. As a result, the geometry shown in Fig. 2 is extended further upstream in the simulation (to –10) solely for computational convenience. The resulting area distribution, with and without a forward centerbody translation (NASA Glenn Research Center wind-tunnel W7's nozzle) is shown in Fig. 4. Note

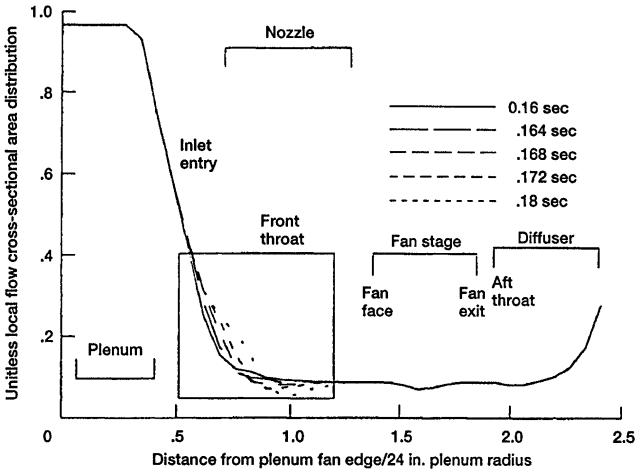

a) Area distribution

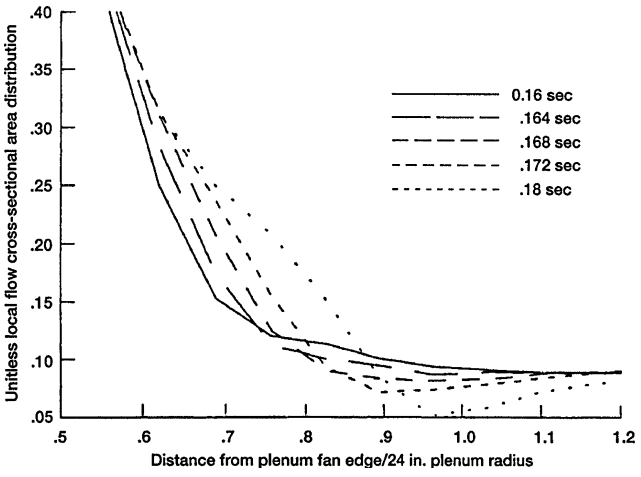

b) Close-up on minimal areas (throats) formed at different times of translation

Fig. 4 Flow cross section: a) note effective choke points (throats) in the flow at selected times during nozzle (front centerbody) translation and b) close-up view.

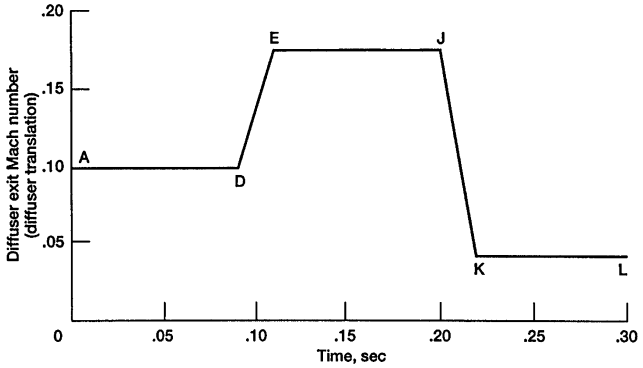

a) Diffuser exit Mach-number schedule simulating rear diffuser translation

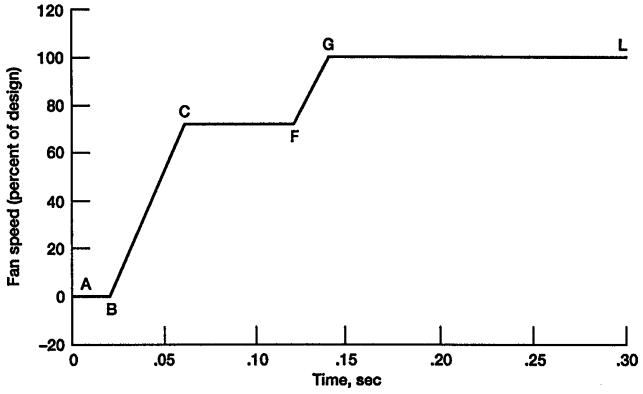

b) Fan speed schedule simulating a startup to quickly get to operating condition

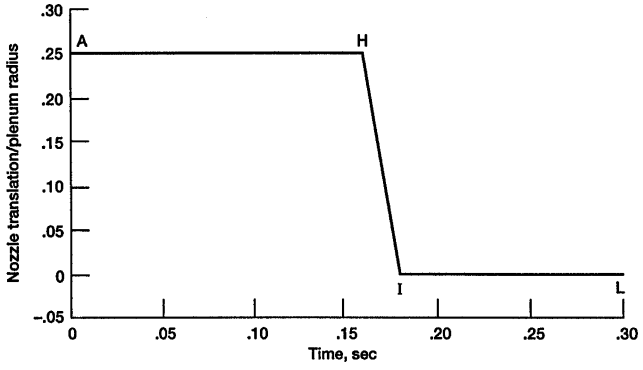

c) Forebody (test cell front nozzle) translation schedule

Fig. 5 Case 1 simulation for design speed and fan face Mach number of 2 (see Table 2 for labels): a) throttling schedule, b) fan speed schedule, and c) nozzle translation schedule.

the changes in effective throats (minimal, cross-sectional flow areas) as the centerbody translates.

Because the effect of a normal shock is of interest, initial downstream boundary conditions are such that a normal shock is created downstream of the second throat. The exit Mach-number boundary condition is reduced, according to the schedule in Fig. 5a, after steady-state fan operation is established in the simulation to force the shock upstream and interfere with normal fan operation. (The effects of that interference are discussed later.) The exit boundary condition specified is the Mach number at the boundary of the model (where the flow exhausts into the aft plenum), which simulates the area changes associated with diffuser (aft centerbody portion) motion. This is the only exit boundary condition chosen to be controlled in the STF model; the corresponding physical effects on other flow variables are reflected in the results.

Because the centerbody move as one piece in the code's design, the exit Mach-number boundary condition changes specified (Fig. 5a) are to simulate the motion of the downstream portion of the centerbody (diffuser), whereas the specified translation is mostly for the nozzle (front centerbody section; see Fig. 5c). So the exit Mach-number schedule represents rear diffuser translation, separate from forebody (front nozzle) translation, and with this, a variety of parameters can be changed to simulate various startup transients.

V. Results and Discussion

Several different cases are examined. In each case, a nozzle motion schedule, a fan speed schedule, and an exit Mach-number schedule are chosen to simulate the startup transient used during steady-state experiments.[12] Again varying the diffuser exit Mach number simulates a throttling. The timescales in the schedules are for simulation convenience (chosen to minimize computing time) and are not the times from the STF experimental research program.[10]

The startup procedure[12] is simulated quickly to sooner reach a point of interest and can be described as follows. With the nozzle and diffuser set at nominal positions, the fan speed is increased to 75% of design. At 75% speed, the diffuser is opened to allow supersonic exit flow. At this condition, the speed could be held constant or increased before starting the inlet. To start the inlet, the nozzle is closed to have supersonic flow in the inlet and finally through the fan.

In each case presented, the motion schedule times from 0.0 to 0.2 s represent the steady-state performance, and times greater than 0.2 s represent the dynamic performance. Local values of Mach number and total pressure are calculated and presented as a function of time (units kept to identify frequencies). Also presented against time for each case is the exit fan total pressure divided by the inlet fan total pressure. Table 2 shows the labels associated with the point in time in the plot of the results when a parameter is changed (A, B, C, etc.). Times that are not initially specified in the schedules get specified when significant changes in the results occur and are also labeled (B′, H′, H″, etc.). These labels highlight the differences between the times in the schedules and the characteristic times for the fan dynamics. The labels also highlight the simultaneous effects in the variables in the other plots.

A. Case 1: Design Speed and Mach 2 at Fan Face

An exit Mach-number (throttling) schedule, a nozzle translation schedule, and a fan speed schedule that simulate the case of operating the fan to design speed with a fan face Mach number of 2 are presented in Fig. 5. In this case (case 1), as with the experimental data, the nozzle and exit Mach number (diffuser position) were held constant until after 75% design speed (simulation time of 0.06 s, labeled C in the figures). At 75% speed, the exit Mach

Table 2 Key parameter actuation and response times as in the figures and Ref. 15

Time, s	Point label
0.000	A
0.020	B
0.045	B′
0.060	C
0.090	D
0.095	D′
0.105	D″
0.110	E
0.115	E′
0.120	F
0.140	G
0.160	H
0.164	H′
0.168	H″
0.172	H‴
0.180	I
0.200	J
0.212	J′
0.220	K
0.300	L

number increased while maintaining constant nozzle position and speed (time of 0.09 to 0.11 s, points D to E in Fig. 5a). The speed was then increased to 100% design speed (time 0.12 to 0.14 s, F to G in Fig. 5b). At design speed, the nozzle was moved to obtain a Mach number of 2 at the fan face (time of 0.16 to 0.18 s, H to I in Fig. 5c). Figure 4 shows the transition to the front throat from the primary throat formed by the fan when it helped accelerate the subsonic flow upstream of it to the supersonic flow downstream of it (note the minima of the curves of Fig. 4b). The flow downstream of the nozzle was fully supersonic until it reached a smaller area or a boundary condition downstream that forced the creation of a shock. This startup transient was followed by the part of the schedule representing steady-state performance of the fan stage (time of 0.18 to 0.2 s, I to J in all parts of Fig. 5). At a time of 0.2 s, the exit Mach number was decreased to represent a throttling of the fan stage (J to K in Fig. 5a). After 0.22 s, the exit Mach number was kept constant as the fan responded to the throttling (K to L in Fig. 5a).

The gradual decrease in exit Mach number that starts at the 0.2 s is akin to throttling down (Fig. 5a). Reducing this downstream Mach number is like closing the exhaust by moving the diffuser or rear centerbody portion forward or by loading the back end of the fan-inlet system. The pressure also changes correspondingly.

The fan-inlet system's response to the already mentioned motion schedule for case 1 is presented in Figs. 6 and 7. The calculated local Mach number (Figs. 6a and 6b) and total pressure (Figs. 6c and 6d) are presented as functions of time. The oscillations at 0.17 s appear because of numerical, and not physical, reasons depending on the selected time steps and grid sizes. These effects can be differentiated from the actual response by evaluating the total pressure ratio plots in Fig. 7. The arrows show the primary path and trends in the maps acknowledging that some smaller and minor bends may be due to numerical errors.

When the exit Mach-number boundary condition is reduced slightly (after 0.2 s according to the schedule in Fig. 5a), a condition results in which a shock sits on the trailing edge of the STF (on the trailing edge of the stator). Because the STF does not contain a constant cross-sectional area, nor the largest one in the flow (but larger than cross sections downstream, from where the shock originated), this shock quickly jumps upstream through the fan under the adverse pressure gradient of the end loading (after 0.2 s as Fig. 6a shows). The shock motion can be traced by noting how long the Mach number (Figs. 6a and 6b) and total pressure (Figs. 6c and 6d) remain constant at the different stations plotted.

When the exit Mach-number boundary condition is decreased by approximately 75% from he steady-state value (the operating point), the fan-inlet system unstarts and goes toward surge. This decrease is akin to tripling the exit static pressure or to reducing the exit corrected weight flow rate by 75%. Note that while the throttling began at 0.2 s (point J in Fig. 5a), the shock does not start going upstream until 0.21 s (point J' in Fig. 6), which indicates a delayed response as the strength of the throttling reaches a point where the fan-inlet system unstarts.

Figures 6c and 6d show the accompanying effect on stagnation pressure. Figures 7a and 7c show the associated performance map of the startup, which can be followed to the operating point and subsequent throttling in Figs. 7b and 7d. When the shock jumps through the fan, the flow at the fan face reaches its maximum rate because the flow is supersonic there. Because the flow rate does not change there (after reaching supersonic), the total pressure ratio increases at a constant rate as the flow reaches a steady-state operating point.

When the throttling is imposed, the Mach number returns to its subsonic value at approximately 0.22 s (point K in Fig. 7). As this throttling continues, oscillations start to occur in the Mach number, flow rate, and total pressure (right after point K in Fig. 7). Plotting these two oscillations with respect to each other results in the limit or surge cycle in Figs. 7b and 7d. The pattern also appears in the map with the Mach number as the abscissa (Fig. 7d).

B. Case 2: Design Speed and Mach 1.5 at Fan Face

The next case simulated was with the same fan and diffuser schedule as was used in case 1. The nozzle was fixed to provide a fan face

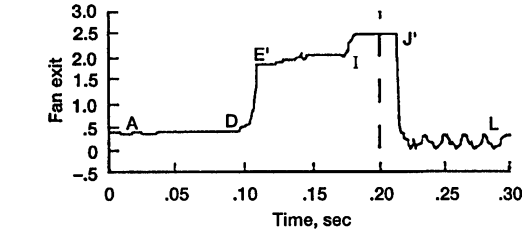

a) Case 1: Mach number at fan exit

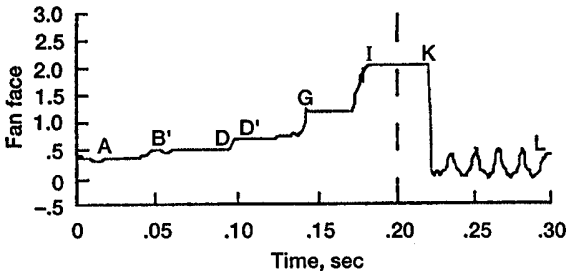

b) Case 1: Mach number at fan face

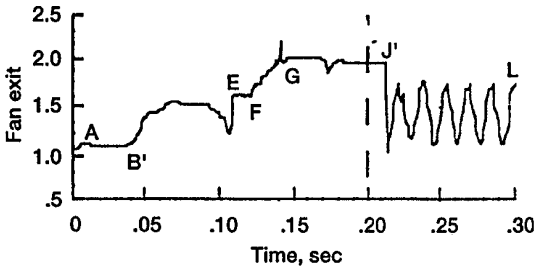

c) Case 1: Total pressure at fan exit

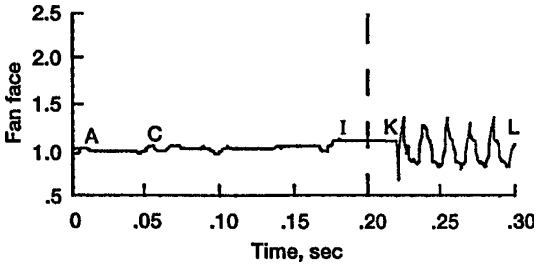

d) Case 1: Total pressure at fan face

Fig. 6 Case 1: Startup transients to design fan speed steady-state operating point (dashed line at 0.2 s), nozzle kept forward for fan face Mach 2, followed by throttling.

Mach number near 1.5 and a combination of similar cross-sectional throat areas (keeping Fig. 4 in mind). In this case, the pressures are constant with time, which means a shock at some location would stay there. However, the pressures in the different locations are not the same, and that difference makes the shock move. Further, similar cross-sectional areas at various locations are possible places that a shock could go (suggesting a low tolerance for geometry changes). The throttling leads to a normal shock moving upstream and to oscillations as in case 1 (Figs. 5–7), but the oscillations are stronger, and the shock actually goes back and forth across the fan. This is a type of supersonic surge (Figs. 8 and 9).

Figure 9d shows the Mach-number cycling at the fan face below and above 1; at the fan exit it cycles at the same frequency but does not go above 1. This suggests that the shock is moving back and forth across the plane of the fan face. During this oscillation, the shock can go as far downstream as across the front part of the rotor, or all of the rotor, or even back to the stator.

Figures 9a and 9c show that this case mirrors case 1 (Figs. 7a and 7c) until point G. From then on, the limited fan face Mach number at which the fan-inlet system is (Fig. 9b) forces a different steady-state operating point to be reached (point J in Figs. 8 and 9).

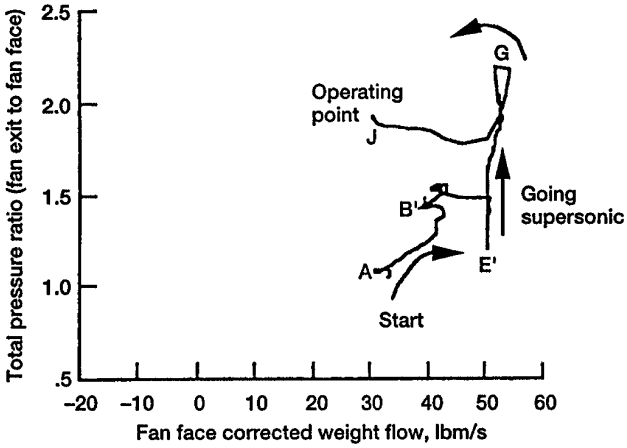

a) Case 1: Total pressure ratio vs corrected weight flow rate at fan entry from start to design operating point

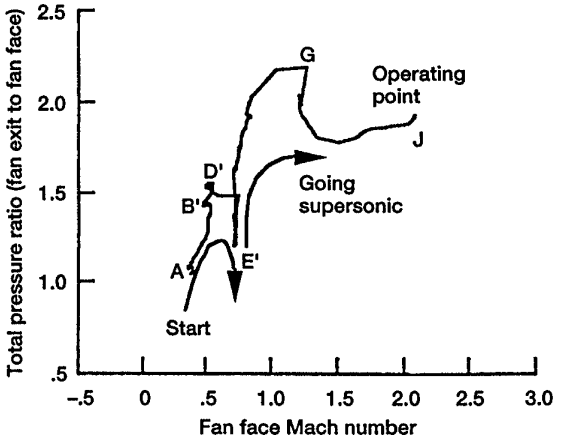

c) Case 1: Total pressure ratio vs Mach number at fan entry—startup to design operating point

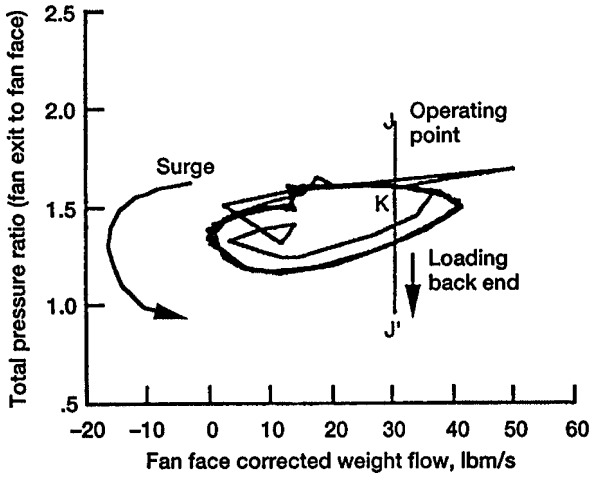

b) Case 1: Total pressure ratio vs corrected weight flow rate at fan entry with rear diffuser Mach number reduced after reaching design operating point

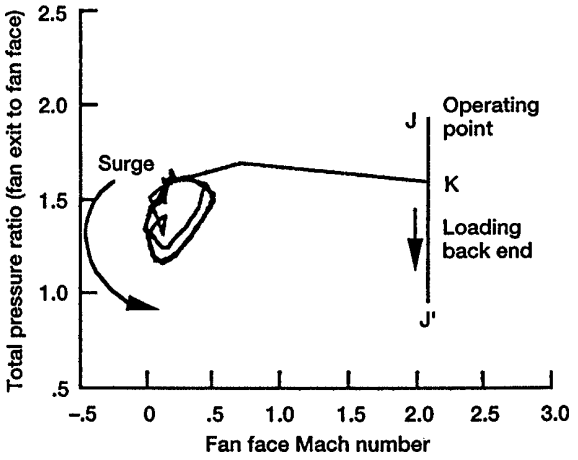

d) Case 1: Total pressure ratio vs Mach number at fan entry with rear diffuser Mach number reduced after reaching design operating point

Fig. 7 Case 1: Dynamic response maps. Note shock moved back to upstream of fan with an oscillation in pressure indicating subsonic surge.

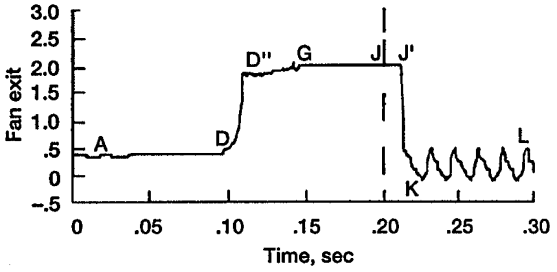

a) Case 2: Mach number at fan exit

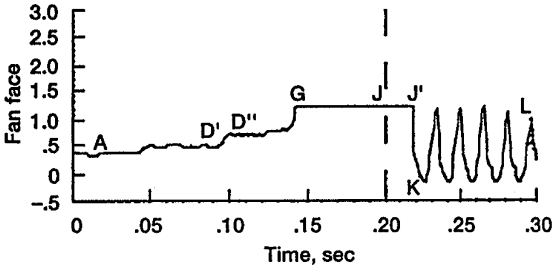

b) Case 2: Mach number as flow enters fan

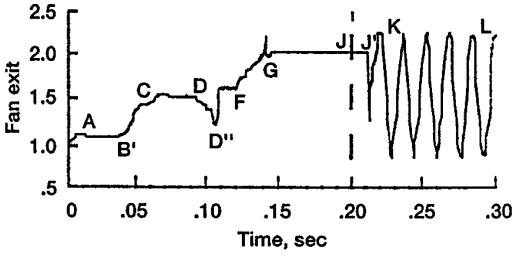

c) Case 2: Total pressure (nondimensionalized) at fan exit

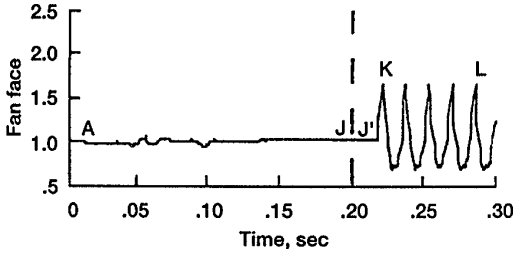

d) Case 2: Total pressure (nondimensionalized) at fan entry

Fig. 8 Case 2: Startup transients to design fan speed steady-state operating point (dashed line at 0.2 s), nozzle kept forward for fan face Mach 1.5, followed by throttling.

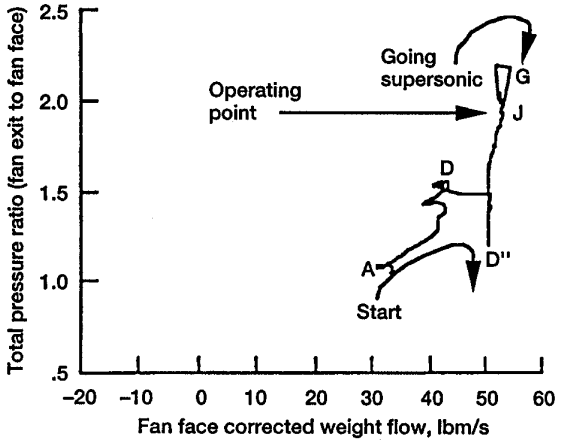

a) Case 2: Total pressure ratio vs corrected weight flow rate at fan entry from start to design fan speed but Mach 1.5 flow entering fan

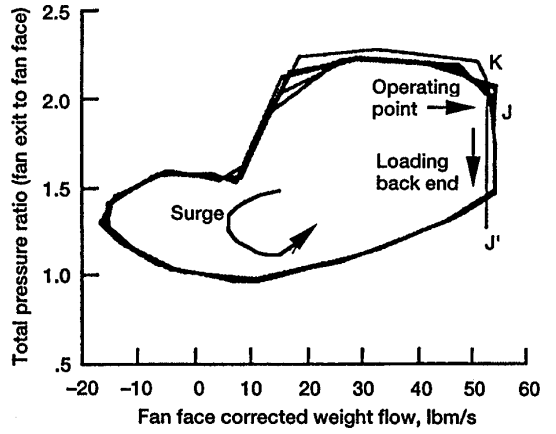

b) Case 2: Total pressure ratio vs corrected weight flow rate at fan entry, where $M = 1.5$, with diffuser Mach number reduced after reaching design fan speed

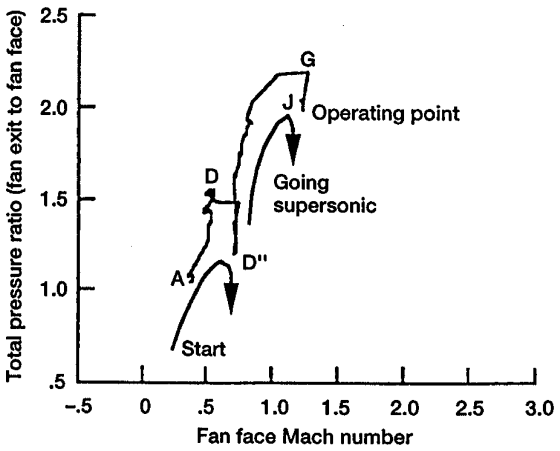

c) Case 2: Total pressure ratio vs Mach number at fan entry from start to design fan speed but Mach 1.5 flow entering fan

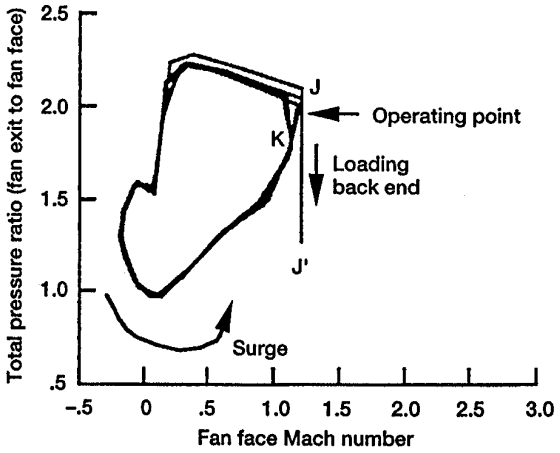

d) Case 2: Total pressure ratio vs Mach number at fan entry with diffuser Mach number reduced after reaching design fan speed but Mach 1.5 flow entering fan

Fig. 9 Case 2: Dynamic response maps. Note shock moved back to upstream of fan but oscillates, going upstream and downstream of the fan indicating supersonic surge.

Note from Figs. 9b and 9d that the surge cycle is very large indicating a very large surge cycle. The Mach numbers and total pressures in Figs. 8 and 9 for this case do not go as high as those in Figs. 6 and 7 for case 1. This indicates that any developing shock in this case will be weaker before the supersonic surge than the case 1 flowfield. This also means that a surge transient has a weaker system through which to propagate, and so the surge cycle can be larger (Fig. 9d vs Fig. 7d).

C. Control and Design Issues

Violent oscillations occur after the inlet unstarts from the back loading. One can infer from this that avoiding unstart will avoid surge. These oscillations, which result from the gradual reduction of downstream Mach number (the specified end boundary condition), simulate the effects of downstream mass flow rate or pressure decreases (throttling) on the fan-inlet combination. The physical event that would cause the unstart and surge represented by these oscillations is the movement of the diffuser, which changes the Mach number and the other flow parameters. The oscillations in the Mach number around the upstream throat imply that the fan-inlet combination tries to restart but cannot. Such oscillations can damage the fan. The oscillations include a flow reversal (e.g., Fig. 9d). With lesser end-Mach-number reductions, oscillations would occur in the simulations, though not always with the periodic flow reversal.

High geometrical sensitivities implying a small stability margin have been observed,[14] and they imply possible difficulties with a variable geometry fan (e.g., an STF design with variable pitch). Some geometric variations could hasten recovery from surge by helping the shock move through the fan quickly and leading the shock to a more stable rest area. The engine control designer or the pilot might not consider sudden jumps favorable, even to hasten shock passage, but these jumps must be acknowledged if geometric variations are in the design. Adding variable geometry capabilities to the fan via blade twist or variable pitch can help if done properly.

Earlier subsonic turbomachinery studies suggested that using bleed could reduce the effects of surge and stall.[13] However, bleed flow had no significant effects on the STF[20] in supersonic surge although the STF can go into subsonic surge. Other means of controlling supersonic surge need to be identified. An in-depth analysis of the effects of bleed needs to be conducted. In any case, bleed might be good to have as an additional control variable (especially for the peace of mind of the STF-using vehicle's pilot or the engine designer—even if largely for subsonic).

The fan can be part of a propulsion system concept that can have additional fan stages, a core engine, one or more compressors, and turbine stages as part of that core, and perhaps an afterburner. Any of these, if not carefully controlled, could cause the dangerous shock behavior observed here. Any one or more could also be used to recover from that behavior. Careful component matching of an STF-based engine is required to avoid undesirable shock behavior.

It is left for the structural dynamicists to examine the effects of the pressure oscillations on the blades. The structural dynamicists might be able to decide what the structural limits of their engine design are from the working pressure of their design. The percentage of this working pressure can be compared with the nondimensionalized pressure plots shown. The percentage of this working pressure is itself a percentage of a design pressure set in the simulation.

VI. Summary

This analytical investigation of supersonic through-flow fan (STF) dynamics was conducted by using an inviscid, quasi-one-dimensional, dynamic model. This study showed that a normal shock could come to rest in various locations in the STF. The locations depend on parameters such as the Mach number far downstream and the front centerbody position. When the back end of the system was loaded with the fan at design speed and the nozzle held forward to yield a Mach number of about 1.5 at the fan face, a shock was made to jump back and forth through part of the fan stage in a supersonic surge. Changes in the timing of the response of the fan-inlet system were observed when geometric variations were introduced.

Separating the STF's rotor and stator could show more possible shock rest locations (e.g., between stator and rotor or on the stator—more likely than on the moving rotor). These shock locations would be affected by the differences in pressure ratios across the STF's rotor compared with the stator. In any case, a preliminary dynamic model of the STF yielded notable results; in particular, a supersonic surge was shown to be possible.

Acknowledgments

The author wishes to thank Bill Bruton and Sue Krosel for their help with the map search routines. The author thanks Carl F. Lorenzo and NASA Glenn Research Center for their support.

References

[1]Mack, R. J., "A Supersonic Business-Jet Concept Designed for Low Sonic Boom," NASA/TM-2003-212435, 2003.

[2]Conners, T., Howe, D., and Whurr, J., "Impact of Engine Cycle Selection on Propulsion System Integration and Vehicle Performance for a Small Quiet Supersonic Aircraft," AIAA Paper 2005-1016, Jan. 2005.

[3]Howe, D., "Improved Sonic Boom Minimization with Extendable Nose Spike," AIAA Paper 2005-1014, Jan. 2005.

[4]Freund, D., and Simmons, F., "Morphing Concept for Quiet Supersonic Jet Boom Mitigation," AIAA Paper 2005-1015, Jan. 2005.

[5]Horinouchi, S., "Conceptual Design of a Low Boom SSBJ," AIAA Paper 2005-1018, Jan. 2005.

[6]Chesnakas, C. J., and Ng, W. F., "Supersonic Through-Flow Fan Blade Cascade Studies," *Journal of Fluids Engineering*, Vol. 125, Sept. 2003, pp. 796–805.

[7]Dang, T. Q., Damle, S. V., and Reddy, D. R., "Throughflow Method for Turbomachines Applicable for All Flow Regimes," *Journal of Turbomachinery*, Vol. 119, April 1997, pp. 256–262.

[8]Franciscus, L. C., "The Supersonic Through-Flow Turbofan for High Mach Propulsion," NASA TM-100114, 1987; also AIAA Paper 87-2050, July 1987.

[9]Schmidt, J. F., Moore, R. D., Wood, J. R., and Steinke, R. J., "Supersonic Through-Flow Fan Design," AIAA Paper 87-1746, Jan. 1987; also NASA TM-88908.

[10]Moore, R. D., Tweedt, D. L., and Chima, R. V., "NASA Lewis Supersonic Through-Flow Fan Program," NASA TM-103248, 1990.

[11]Moore, R. D., and Tweedt, D. L., "Aerodynamic Performance of a Supersonic Through-Flow Fan Rotor," NASA TP-3115, 1991.

[12]Moore, R, D., Schmidt, J. F., and Tweedt, D. L., "Aerodynamic Performance of a Supersonic Through-Flow Fan Stage," NASA TP-3308, 1993.

[13]Greitzer, E. M., "Review—Axial Compressor Stall Phenomena," *Journal of Fluids Engineering*, Vol. 102, June 1980, pp. 134–151.

[14]Greitzer, E. M., "Surge and Rotating Stall in Axial Flow Compressors, Parts I and II," *Journal of Engineering for Gas Turbines and Power*, Vol. 98, No. 2, April 1976, pp. 190–217.

[15]Day, I. J., Greitzer, E. M., and Cumpsty, N. A., "Prediction of Compressor Rotating Stall," *Journal of Engineering for Gas Turbines and Power*, Vol. 100, No. 1, 1978, pp. 1–12.

[16]Sugiyama, Y., Tabakoff, W., and Harried, A., "J85 Surge Transient Simulation," *Journal of Propulsion and Power*, Vol. 5, No. 3, 1989, pp. 375–381.

[17]Varner, M. O., Martindale, W. R., Phares, W. J., Kneile, K. R., and Adams, J. C., Jr., "Large Perturbation Flow Field Analysis and Simulation for Supersonic Inlets," NASA CR-174676, Sept. 1984.

[18]Cole, G. L., and Richard, J. C., "Supersonic Propulsion Simulation by Incorporating Component Models in the Large Perturbation Inlet (LAPIN) Computer Code," NASA TM-105193, Dec. 1991.

[19]Richard, J. C., "Preliminary Results from Quasi-One-Dimensional Dynamic Modeling of a Supersonic Throughflow Fan System," NASA TM 106317, July 1994 (limited distribution until 1999).

[20]Chicatelli, A. K., and Richard, J. C., "Reduced Order Linear Modeling of Supersonic Compression & Propulsion System Dynamics," NASA TM 106090, March 1993 (limited distribution until 1998).

[21]Hart, C. E., "Function Generator Sub-Programs for Use in Digital Simulations," NASA TM X-71526, Jan. 1974.

[22]Chima, R. V., "RVCQ3D—Rotor Viscous Code Quasi-3-D, User's Manual and Documentation," ver. 303, NASA Glenn Research Center, Cleveland, OH, March 1999.

[23]Chima, R. V., "Viscous Three-Dimensional Calculations of Transonic Fan Performance," *CFD Techniques for Propulsion Applications, AGARD Conference Proceedings*, No. CP-510, AGARD, Neuilly-Sur-Seine, France, 1992, pp. 21-1–21-19; also NASA TM-103800.

[24]Chima, R. V., "Swift—Multiblock Analysis Code for Turbomachinery, User's Manual and Documentation," ver. 300, NASA Glenn Research Center, Cleveland, OH, Sept. 2003.

[25]Chima, R. V., "Calculation of Tip Clearance Effects in a Transonic Compressor Rotor," *Journal of Turbomachinery*, Vol. 120, No. 1, 1998, pp. 131–140.